Numerical Modelling of Pavement Materials

I M A Gledhill[1] **, J M Greben**[2] **and R de Villiers**[2]

[1]Defence, Peace, Safety and Security Unit, [2]Built Environment Unit,
CSIR, PO Box 295, Pretoria 0001 South Africa

E-mail: igledhil@csir.co.za

Abstract. Gravel aggregates form the foundation of road and rail pavements, but comparatively little work has been performed on characterising the bulk properties of aggregates composed of particles with different shapes. In the current project, the aspect ratio, angularity, and surface texture of natural quarry output and recycled materials are being quantified through laser scanning, and the bulk properties are determined in the laboratory. In addition, a numerical approach is being taken to understand the influence of the particle properties on macroscopic behaviour. Both Discrete Element Methods and physics engines are being employed. In this paper, preliminary results for the physics engine model, for regular solid shapes, are presented. A simple uniaxial test is simulated. No fracturing is modelled. The elastic modulus is measured during consolidation and shown to increase with increasing angularity index, until void fraction is minimised, except in the case of cubes, which align and prevent further compression at relatively low stresses.

1. Introduction

In the development of South Africa and its economy, transport infrastructure plays a critical role. This infrastructure is strongly influenced by the quality and cost of the pavements of roads and airfields and the support of rail tracks. By incorporating recycled material in road pavement aggregates [1] [2] costs can be reduced; however, this should not come at the expense of road performance. In order to ensure that new road pavements meet performance criteria, stress tests are carried out on proposed road materials, and are assisted by new techniques to characterize the shape and surface properties of rock aggregates. Within the pavement engineering community, there is a growing concern about the traditional experience-based empirical methods and procedures for quantifying shape (*e.g.* Flatness and Elongation ratio) and surface properties of rock aggregates. The CSIR has introduced advanced materials characterisation using new laser scanning techniques to analyze the properties of aggregates. At the same time numerical work has started to simulate stress tests using both Discrete Element Methods (DEM)[3][4][5] and more novel physics engines. The current paper deals with the latter. The physics engine chosen for present purposes is PhysX™ [6]. Physics engine software was developed to take advantage of the rapid development of Graphical Processing Units (GPUs) prompted by the fast-growing market for animation, visualisation, robotics and virtual environments. The purpose of these studies is to relate the bulk properties road materials to particle shape. PhysX has already been applied successfully in an application to breakwater structures [7].

In this investigation we use PhysX to simulate consolidation tests. The setup for the simulations is to confine the road material to a rigid cylinder with a fixed base and a top (platen), which can move under the imposed forces. Each particle of the aggregate is modelled by a polyhedron, which allows particles of different shape and angularity. After the material has equilibrated during setup, weights of

different mass are placed on the platen and the axial strain is determined from the relative decrease in height. In the next sections we will present the first results of these simulations. An important initial task is to demonstrate that the approach is feasible and that the results are sufficiently realistic.

After we have reported some of the explicit calculations in the next section, we present some conclusions and suggest further steps to improve the simulations.

2. Physics engine model

The components of a physics engine such as PhysX are object representation, collision detection, collision processing, and particle kinematics. Each body is represented by a tetrahedral mesh model. It is important that PhysX provides the ability to manage collisions between polyhedral units, since in most DEM methods, particles are approximated by multiple spheres – an approach which is unsuitable for this application, in which flat planes are in sliding contact.

Rigid body collisions are based on the constraint models of Hahn [8]. Collision detection is based on a scheme of bounding boxes, and a contact graph keeps a record of interactions between moving bodies and immovable boundaries. In a collision, particle boundaries may overlap or "overshoot". To manage overshoot, a skin width for maximum overlap is specified by the user, and the collision is integrated back in time to until the overlap is less than the skin width, using the contract graph. For each collision, a calculation of contact normals, normal velocities, and tangential velocities before and after the collision takes place, and provides updated position and orientation for each particle subject to conservation equations and constraints. Static and dynamic friction and a coefficient of restitution for the objects are formulated within the constraints. Chatter is controlled by a "sleep" mode: particles are deactivated, and velocities are unchanged, when the kinetic energy or velocity in a collision falls below a threshold. This mode allows a collection of particles to rest in equilibrium, instead of indefinitely adjusting due to minor collisions.

3. Uniaxial test model

Natural aggregates are characterised by particle size distributions measured with graded sieve sizes. For development purposes, all particles used for the following results are the same size and shape in each simulation, and are the five regular solids, and the sphere. Each particle is characterised by the diameter D, where D is the length of a side of a square grid through which the particle can pass. For the regular solids, D is the diameter of the midsphere, defined as the sphere which is tangent to every edge. The particles have a density of 2.5×10^3 kg m^{-3}, which is in the range of rock densities. Coefficients of friction and restitution are discussed below.

The consolidation test [9], with rigid steel cylinder walls, is frequently employed for soil testing, in which the presence of water is a critical factor. In laboratory uniaxial and triaxial testing, a flexible elastic membrane forms the cylinder walls, and a confining stress is produced by applying a regulated air pressure in a surrounding pressure chamber. In the uniaxial simulation model, rigid confining walls are used, and no water is modeled. The following assumptions often used in laboratory testing are inapplicable, and are the reasons for undertaking numerical rather than theoretical models. The particle size (sieve size 26.5 mm) is significant in comparison with the inner radius of the cylinder (15 cm) and the initial cylinder height (15 cm), and the material is inhomogeneous. For simple laboratory experiments, it is assumed that stress is uniform across the confining surfaces, and that there are no stress concentrations in the sample. However, in the simulation, at the wall, floor, and platen boundaries, the walls are in contact with local asperities. In addition, the local void fraction is higher at the walls than in the bulk of the aggregate, since stones are excluded by the presence of the walls. As in all granular media, stress is transferred in force chains between particles in contact.

In the physics engine model there is no provision for controlled strain experiments, as used in the laboratory, and controlled stress is employed. Stress is applied by loading the platen with weights. Each mass is increased by a constant percentage from the last one. In the data shown here, the increase is 2% per weight. The time step used for the particle sizes modeled here is 1 ms. A settling time of 1000 time steps is allowed after each weight is placed.

Particles are loaded into the cylinder by hand in the laboratory, under controlled conditions. In the simulation, particles are loaded into the cylinder layer by layer. One layer is constructed on a hexagonal horizontal grid based on the radius of the particles, with a random orientation for each particle. The *m*th layer in loading is allowed to settle for a time 2000+100 *m* time steps. Initial conditions are different for each loading.

Stones are laid until the height of the centre of mass of the top stone is 5 cm above the top of the cylinder. Stones are then removed (scalped) to trim the top layer so that no stone protrudes above the cylinder height. In the laboratory, the sample may be conditioned by vibration or impact. In the simulation, the compression procedure is started after trimming the top layers. The platen is brought into contact with the new top layer and released under gravity. Weights are added (Figure 1), and 1000 time steps allowed for settling. The height of the platen base is recorded.

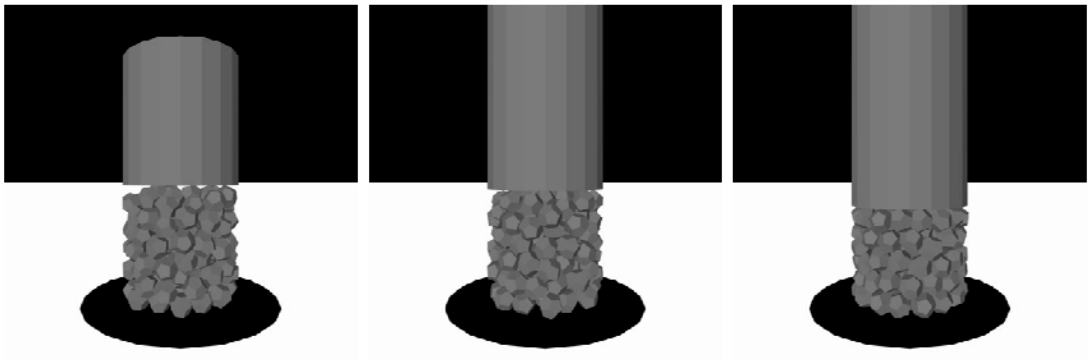

Figure 1. A time series of scenes showing dodecahedra during consolidation. The cylinder is indicated by its shadow only.

A limitation of the method is observed to be that as the weights are added, they collide and may exert time-dependant stress on the stones. The process is discernible in the results, as discussed below.

In laboratory triaxial and uniaxial tests, a granular material will usually exhibit failure in the stress-strain curve in a manner similar to a brittle material, as friction is overcome and the material slips along a plane. The membrane allows horizontal dilation to occur. In a rigid cylinder, dilation cannot take place, and a constant strain is reached. The PhysX model behaves in a similar way, but experience shows that particles start to chatter or spin in an unphysical manner at high stresses. Increasing the energy lost in collisions, through the coefficients of restitution and friction, reduces the chatter. It should be noted that the stones in this simulation will behave like particles in a gas, and the mean speed will increase under compression, unless a mechanism is provided for the loss of kinetic energy. In a gravel aggregate, these mechanisms are energy conversion to material heating via fracture and material deformation. Fracture is not simulated in the current PhysX model. Following Mattutis *et al.* [10] the coefficient of restitution for all materials was set to zero in order to provide a mechanism for the "absorption" of energy.

In this preliminary study, coefficients of static and dynamic friction between all materials are zero. Sleep thresholds are 0.15 ms^{-1}, 3.0 s^{-1} and 0.05 J for translation and rotational velocity and kinetic energy respectively, and the skin width is 0.1 mm.

4. Particle angularity index

The methodology of Tutumluer [5] is followed in calculating the angularity index *A*. The particle shape is projected along each of the principal axes and the *n*-gon outline extracted; the standard value $n = 24$ was used. The internal vertex angles α_i are found. The differences $\beta = \alpha_j - \alpha_{j-1}$, with j periodic, are found. The frequency $P(e)$ in 10º intervals is calculated.

We define for *i=1..3* dimensions, with projected area a_i, angularity A:

$$A = \left[\sum_i a_i \left(\sum_{e=0^\circ}^{170^\circ} eP(e)\right)_i\right] [\sum_i a_i]^{-1}.$$

5. Preliminary results

Figure 2 shows sample stress and strain for octahedra. It has been verified that different initial conditions, as illustrated, provide similar results in the linear range. Three regions can be identified with the aid of inspection of the behaviour of the particles in the PhysX scenes. For $0.0 < \varepsilon < 0.1$, approximately, the void fraction under the platen is decreased. For $0.1 < \varepsilon < 0.2$, approximately, a linear region of consolidation occurs. For $\varepsilon > 0.2$, approximately, the void fraction has reached its minimum, and the particles start to chatter and rotate. For each particle shape used, these regions have been identified and the slopes of the linear region of consolidation have been calculated.

In Figure 3 and Figure 4, data for the regular solids are compared (spheres (f1), cubes (f6), octahedra (f8), dodecahedra (f12) and icosahedra (f20)). Figure 5 shows the slope *E*, the elastic modulus, in the linear range as a function of angularity index.

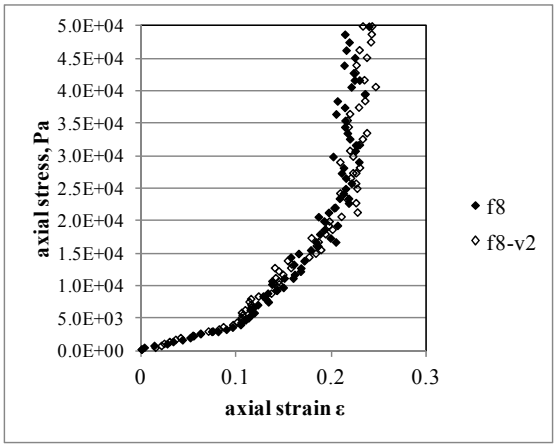

Figure 2. Stress-strain relationship, octahedra, two different initial conditions.

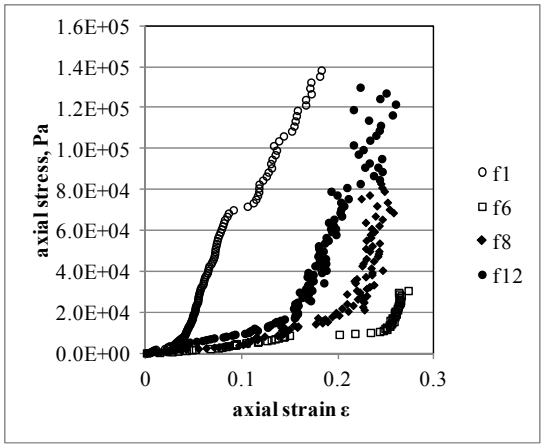

Figure 3. Sample stress-strain relationships for spheres (f1), cubes (f6), octahedra (f8) and dodecahedra (f12)

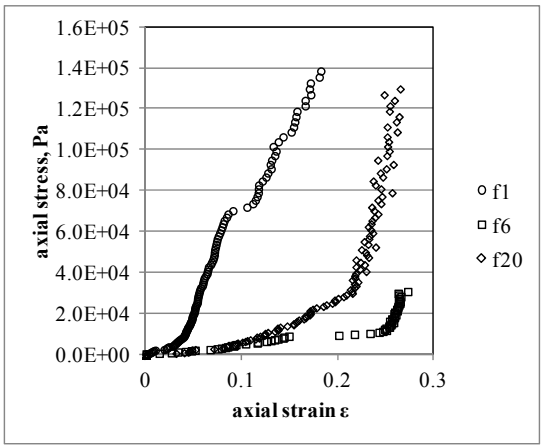

Figure 4. Sample stress-strain relationships, (f1 and f6 included for comparison).

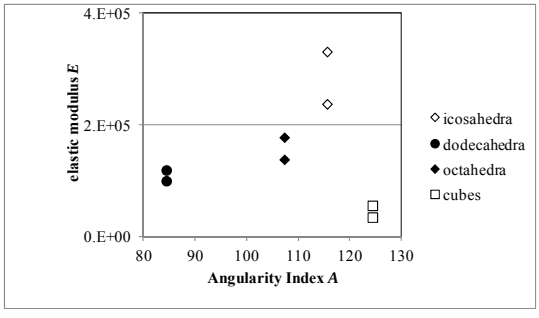

Figure 5. *E* as a function of *A*. Two initial configurations are shown for each shape.

Significant jumps occur, for example, for spheres (figure 3, f1, at 70 kPa). From observing the simulation (as in figure 1) it is seen that these are associated with events where particles slip suddenly into a new configuration; the event appears significant because the system size is small (there are between 100 and 200 particles in these simulations, depending on the shape used).

For cubes (figure 3) it will be noticed that after the linear range, the stress increases sharply while the strain remains approximately constant. At this stage, the cube faces are aligned with the floor, no further compression can take place, and the void fraction has reached the minimum for that initial configuration. Tetrahedra (f4) proved to be difficult to model. This is at present attributed to the small angles at the vertices of tetrahedra which are able to pass through each other within the 1 ms time step used; the hypothesis is to be tested in further numerical experiments.

The elastic modulus is compared with the angularity index in figure 4. For dodecahedra, octahedra and icosahedra, E increases with A. Cubes exhibit a much lower value of E. This may be attributable to the orientation and packing of cubes in columns, which transmit forces only in the direction of the uniaxial compression; an orientational study of the particles is to be conducted to check this hypothesis. Alternatively, it may be related to the manner in which A has been defined.

6. Conclusions and further work

In this set of shape-related physics engine simulations, the elastic modulus of a set of regular polyhedral particles is measured in uniaxial tests. At low stresses, void fraction under the platen is decreasing; and at high stress, particles can cross significant distances in one time step and start to leak through other particle asperities or across barriers; particles also start to chatter or spin at high stress and minimum void fraction. In the intermediate linear range, the elastic modulus can be calculated and increases with the angularity index, except for cubes. This is consistent with current laboratory observations and practice in using aggregates with angular shapes, rather than rounded particles, in unbound pavement layers.

This study was confined to smooth frictionless particle surfaces for regular solids. The next steps are the modeling of simple Coulombic friction effects, and surfaces with a quantified surface texture index. Calibration of model parameters is then essential for validation of the model against physical behaviour [11]. Related work on more accurate, but slower and more computationally demanding, Discrete Element Models is being undertaken, in which these preliminary results with the physics engine will provide guidelines. In future tasks, the shapes of laser-scanned particles from quarry samples will be used.

References

[1] Anochie-Boateng J K, Komba J and Mvelase G M 2011 *Proc. Int. Road Fed., Int. Road Congress (Moscow, Russia, 22-24 November 2011)*

[2] Anochie-Boateng J, Komba J and Tutumluer E 2012 *Am. Soc. Civil Eng. J. Transportation Engineering* **138** 1006-1015

[3] Latham J-P, Munjiza A and Lu Y 2002 *Powder Technology* **125** 10-27

[4] Munjiza A *Computational Mechanics of Discontinua* 2011 (New York: John Wiley and Sons)

[5] Tutumluer E, Huang H, Hashash Y and Ghaboussi J 2007 *Proc. Am. Railway Eng. And Maintenance-of-Way Assoc. Conference 2007*

[6] NVIDIA 2012 *PhysX* www.nvidia.com, accessed March 2012

[7] Gledhill I M A, Greben J M, de Villliers R and Cooper A K 2012 *Proc. 8th South African Conf. on Computational and Applied Mechanics, SACAM 2012*

[8] Hahn J K 1988 *Proc. 15th Ann. Conf. on Computer Graphics and Interactive Techniques SIGGRAPH 88*, 299-308

[9] Am. Soc. for Testing and Materials 1998 Standard Test Method D 4186-89

[10] Mattutis H-G, Ito N and Schinner A 2003 *Kôkyûroku* **1305** 89-99

[11] Coetzee C J and Els D N J 2009 *J. Terramechanics* **46** 15-26